Catalysis Today 146 (2009) 50–56

Contents lists available at ScienceDirect

Catalysis Today

journal homepage: www.elsevier.com/locate/cattod

Hydrogen production via partial oxidation and reforming of dimethyl ether

Qijian Zhang [a,*], Feng Du [a], Xinxin He [a], Zhao-Tie Liu [b], Zhong-Wen Liu [b,**], Yingchun Zhou [a]

[a] *School of Material and Chemical Engineering, Liaoning University of Technology, No. 169 Shiying Street, Guta District, Jinzhou, Liaoning 121001, China*
[b] *Key Laboratory of Applied Surface and Colloid Chemistry, Ministry of Education, and School of Chemistry & Materials Science, Shaanxi Normal University, Xi'an 710062, China*

ARTICLE INFO

Article history:
Available online 18 February 2009

Keywords:
DME
Partial oxidation
Reforming
Hydrogen production
Rh
Alkali metal nitrates

ABSTRACT

The catalytic partial oxidation and reforming of dimethyl ether (DME) over composite catalysts composed of 6 wt%Ni/Al_2O_3 and noble metal supported on Al_2O_3 were investigated for the production of hydrogen under ambient pressure. Results indicate that Rh/Al_2O_3 had better performance than Pt/Al_2O_3 for the titled reaction. The modification of Rh/Al_2O_3 with different contents of alkali metal nitrates, i.e., $LiNO_3$, $NaNO_3$, and KNO_3, was comparatively studied. The N_2 adsorption/desorption results showed that both the surface area and pore volume of the Rh/Al_2O_3 obviously decreased with the increase of the content of the modifiers. Moreover, the pore size distribution of Rh/Al_2O_3 was significantly changed by the addition of $LiNO_3$. Irrespective of the modifiers, there were no diffractions assigned to Rh by XRD analysis. By the addition of less than 5 wt% Na into Rh/Al_2O_3, hydrogen yield was obviously increased while DME conversion was always 100%. When the content of Li in Rh/Al_2O_3 was less than 5 wt%, the effect of modifier on both DME conversion and hydrogen yield was negligible. However, the stability of the catalyst indicated either by DME conversion or by hydrogen yield was apparently decreased when the content of Na or Li in Rh/Al_2O_3 was greater than 5 wt%. Even at a lower content of 2.5 wt%, the addition of KNO_3 into Rh/Al_2O_3 deteriorated the stability of the catalyst although there was basically no effect on the initial hydrogen yield and DME conversion. Based on the characterization results and the possible reaction networks, these experimental phenomena were tentatively explained as the electronic promotional effect of alkali metal nitrates on Rh and the structural effects of the modifiers on the pore properties of the catalyst.

1. Introduction

With the exhausting of fossil fuel reserves and the more and more rigorous requirement on the environmental protection, a clean and renewable energy carrier is under hunting. Hydrogen has been considered as the most promising one because of its non-contamination, universal existence and ease availability. A "hydrogen economy" is under construction. However, to realize the hydrogen economy, a series of obstacles must be removed, in which the storage, transportation and distribution of hydrogen are extremely important. Hydrogen is the lightest element on earth whose weight/volume ratio is very low even when it is compressed to high pressure. In addition, hydrogen is a dangerous gas because it is very volatile and easy to leak out, and it will explode when mixed with air. Currently, quite a few methods for hydrogen storage are in development, including high pressure tank, metal hydrides, chemical hydrides, and the recently proposed carbon nanotubes. However, all the above methods suffer from either low hydrogen-storage density or high cost. Thus, it is more suitable to store hydrogen in some compounds, named H_2-carriers, and release it on-site. The possible candidates as a H_2-carrier include CH_3OH, CH_3OCH_3, NH_3, etc., whose hydrogen contents are 12.5 wt%, 13 wt% and 17.6 wt%, respectively. Due to their toxicity, corrosion and bad smells, CH_3OH or NH_3 cannot serves as a safe and convenient H_2 carrier. Dimethyl ether (DME) is a more promising candidate because it is inert, non-carcinogenic, non-mutagenic, non-corrosive, and virtually non-toxic [1,2]. Furthermore, DME has been recognized as a multisource clean fuel because it can be manufactured from oil, coal, natural gas, coal-bed gas, biomass, etc., via the gasification route. More importantly, the direct production of DME from syngas is more economically profitable and thermodynamically favorable than methanol synthesis. If biomass is taken as the raw material, the production route will be a sustainable one. Last but not least, DME requires less cost intensive infrastructure for transport and storage because the existing LPG infrastructures can be directly used for handling DME due to their similar physical properties.

Then the focused problem lies in how to release H_2 from DME. Generally, there are two basic methods for producing hydrogen from DME, i.e., steam reforming of DME (SRD, Eq. (1)), and partial

---

[*] Corresponding author. Tel.: +86 416 4199 590.
[**] Corresponding author. Tel.: +86 29 8530 3200; fax: +86 29 8530 7774.
E-mail addresses: zhangqijian@tsinghua.org.cn (Q. Zhang), zwliu@snnu.edu.cn (Z.-W. Liu).

0920-5861/$ – see front matter © 2009 Elsevier B.V. All rights reserved.
doi:10.1016/j.cattod.2009.01.026

oxidation of DME (POD, Eq. (2)). Both of them attracted attention just in recent few years

$$CH_3OCH_3 + 3H_2O = 2CO_2 + 6H_2, \quad \Delta H = 135\ \mathrm{kJ\,mol^{-1}} \qquad (1)$$

$$CH_3OCH_3 + \tfrac{1}{2}O_2 = 2CO + 3H_2, \quad \Delta H = -37\ \mathrm{kJ\,mol^{-1}} \qquad (2)$$

As shown in Eq. (1), 6 moles of hydrogen can be produced by converting 1 mole of DME in SRD. Moreover, SRD can be carried out at relatively low reaction temperature of about 300 °C. Thus, much attention has recently been paid on hydrogen production via SRD [3–8]. However, SRD is an intensively energy-consuming process because of its highly endothermic nature. On the contrary, as shown in Eq. (2), the POD is a mildly exothermic reaction, which can produce hydrogen with a very high space yield. Unfortunately, the POD was very less studied [2,9–12].

Under the typical POD conditions, the decomposition of DME into CH_4, CO, and H_2 occurs easily so that the efficiency of hydrogen production decreases due to the formation of CH_4. Moreover, the combustion of DME besides POD can also occur, to a certain degree, forming H_2O and CO_2. Thus, hydrogen yield should be improved by presenting a reforming catalyst after the POD catalyst. Indeed, it was demonstrated that hydrogen yield was significantly increased after the addition of Ni/MgO (catalyst for reforming reactions) under Pt/Al_2O_3 (POD catalyst) in our precious works [10,11]. In this work, hydrogen production via partial oxidation and reforming of DME were studied by optimizing the POD catalyst of Rh/Al_2O_3 with alkali metal nitrates, which was combined with Ni/Al_2O_3, the reforming catalyst. The significant effect on both the DME conversion and hydrogen yield by adding different amounts of alkali metal ions into Rh/Al_2O_3 was tentatively explained based on the characterization results.

2. Experimental

2.1. Catalyst preparation

The POD catalysts, i.e., 0.5 wt%Pt/Al_2O_3 or 0.2 wt%Rh/Al_2O_3, were prepared by impregnating the desired amount of H_2PtCl_4 or $RhCl_3$ (Shanghai July Chemical Co., Ltd.) onto home-made γ-Al_2O_3 (by precipitation of $Al_2(SO_4)_3$ with $NH_3{\cdot}H_2O$ and calcined at 800 °C for 3 h, BET surface area = 235.1 m^2/g), respectively. The modification of 0.2 wt%Rh/Al_2O_3 with $LiNO_3$, $NaNO_3$, or KNO_3 was also carried out via impregnation method by using the corresponding nitrate as a precursor. The final POD catalysts were obtained after calcination at 500 °C for 3 h. The 6 wt% Ni/Al_2O_3 catalyst for reforming reactions was prepared by impregnating $Ni(NO_3)_2$ onto the home-made γ-Al_2O_3 as mentioned above, followed by drying, and calcination at 800 °C for 3 h. Before use, all the catalysts were pressed and crashed to 20–40 mesh.

2.2. Activity evaluation

Partial oxidation and reforming of DME were carried out in a fixed-bed continuous-flow quartz tube reactor under ambient pressure. For each run, 0.3 g of each catalyst thoroughly mixed with 0.6 g of inactive silica sands as a diluent was loaded into the reactor. The reforming catalyst, 6 wt%Ni/Al_2O_3 was always located under the POD catalyst to construct a dual bed catalysts system. Before reaction, the catalyst was reduced in a flow of hydrogen (H_2/Ar = 1/1) at 700 °C for 30 min, and then purged by pure Ar for 10 min. DME and O_2/Ar were fed into the reactor separately with the standard composition of DME/O_2/Ar = 35/17/78 ml/min (STD). After condensing water in a cold trap, the effluent was analyzed with two on-line gas chromatographs (GCs). One GC equipped with a TDX-01 column was used for the analysis of CO, CO_2, CH_4, and H_2 with a thermal conductivity detector (TCD). The other GC was equipped with a Porapak N column for the analysis of DME, CH_4, and other hydrocarbons with a flame ionization detector (FID). The DME conversion, hydrogen yield, and C-containing product yield were calculated according to the following equations:

$$\text{DME conv.}\,(\%) = \left(1 - \frac{\mathrm{DME}_{(\text{mmoles/min,out})}}{\mathrm{DME}_{(\text{mmoles/min,in})}}\right) \times 100 \qquad (3)$$

$$\text{Hydrogen yield}\,(\%) = \frac{\mathrm{H}_{2(\text{mmoles/min,out})} \times 2}{\mathrm{DME}_{(\text{mmoles/min,in})} \times 6} \times 100 \qquad (4)$$

$$C_n\ \text{yield}\,(\%) = \frac{C_{n(\text{mmoles/min,out})} \times n}{\mathrm{DME}_{(\text{mmoles/min,in})} \times 2} \times 100 \qquad (5)$$

2.3. Catalysts characterization

X-ray diffraction (XRD) patterns were obtained on a XRD-7000 X-ray diffractometer (SHIMADZU) with a Cu Kα radiation operated at 40 kV and 30 mA. The XRD patterns were collected from 20° to 70° (2θ) at a scan rate of 2°/min.

The pore structure properties of the catalysts were measured on an ASAP-2020M system (Micromeritics) with nitrogen adsorption at 77 K. The samples were degassed at 300 °C for 5 h before analysis.

3. Results

3.1. Comparison of the performance of Pt/Al_2O_3 and Rh/Al_2O_3

Generally, noble metal-based catalyst is active for the POD reaction. In this work, it was supposed to play the role of suppressing the decomposition and total oxidation as well as catalyzing partial oxidation of DME. Firstly, 0.5 wt%Pt/Al_2O_3 and 0.2 wt%Rh/Al_2O_3 combined with the reforming catalyst of 6 wt%Ni/Al_2O_3 were comparatively investigated for the titled reaction. As shown in Fig. 1, DME conversion was basically 100% over both of the catalysts along the time on stream (TOS) of 6 h. When the product yield was concerned, the distributions of C-containing products obtained over the catalysts were very similar (Fig. 2). These results indicate that both Pt/Al_2O_3 and Rh/Al_2O_3 are active and stable POD catalyst. With the respect to H_2 yield, Rh/Al_2O_3 showed a slightly better performance than Pt/Al_2O_3 (77% vs. 75% at TOS of 5 h, Fig. 1). In considering the lower metal loadings of Rh/

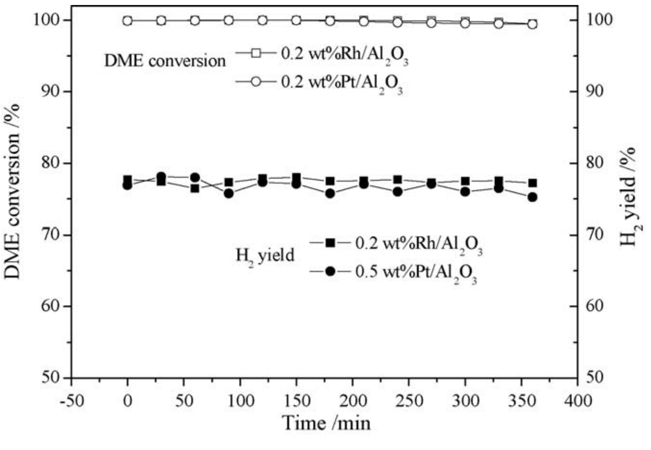

Fig. 1. DME conversion and H_2 yield over noble metal supported on Al_2O_3 combined with 6 wt%Ni/Al_2O_3 catalysts under the reaction conditions of T = 700 °C, P = 1 atm, and DME/O_2/Ar = 35/17/68 ml/min.

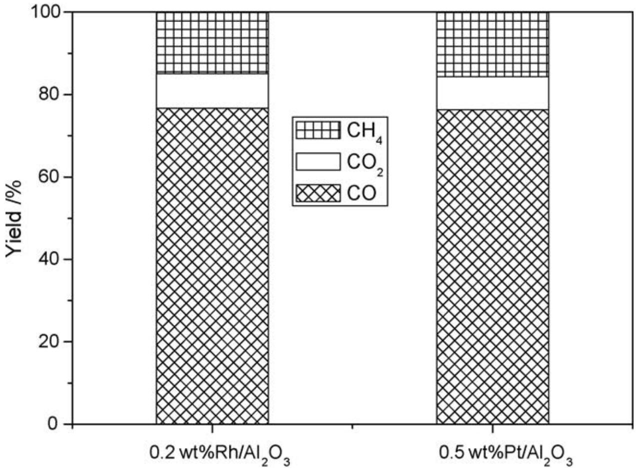

Fig. 2. Distribution of C-containing products over noble metal supported on Al_2O_3 combined with 6 wt%Ni/Al_2O_3 catalysts at TOS of 5 h under the reaction conditions of T = 700 °C, P = 1 atm, and DME/O_2/Ar = 35/17/68 ml/min.

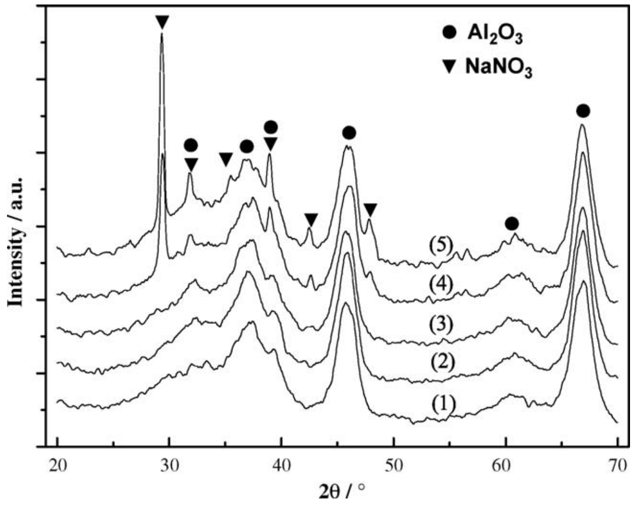

Fig. 3. XRD patterns of the fresh catalysts. (1) 0.2 wt%Rh/Al_2O_3, (2) 2.5 wt%Na–0.2 wt%Rh/Al_2O_3, (3) 5 wt%Na–0.2 wt%Rh/Al_2O_3, (4) 7.5 wt%Na–0.2 wt%Rh/Al_2O_3, and (5) 10 wt%Na–0.2 wt%Rh/Al_2O_3.

Al_2O_3 than Pt/Al_2O_3, Rh/Al_2O_3 should be a better POD catalyst than Pt/Al_2O_3. Based on the definition of hydrogen yield, it can be further increased by either optimizing the POD catalyst or reforming catalyst. In this work, we try to do this by modifying Rh/Al_2O_3, the POD catalyst, with alkali metal nitrates.

3.2. $NaNO_3$ modification of Rh/Al_2O_3

A series of $NaNO_3$ modified 0.2 wt%Rh/Al_2O_3 catalysts (Na content = 2.5 wt%, 5 wt%, 7.5 wt%, and 10 wt%) were prepared and their XRD patterns are shown in Fig. 3. For all the catalysts, there were no diffraction peaks of Rh appeared, among which the strongest peak should appear at $2\theta = 41^\circ$, indicating that Rh was dispersed very well on the supports and its dispersion was not affected significantly by the modification of sodium salt. The peaks at 2θ of ca. 37°, 39°, 46°, 61°, and 67° for the modified and unmodified Rh/Al_2O_3 catalysts were the characteristic diffractions of γ-Al_2O_3. These results indicated that the bulk structure of γ-Al_2O_3 was still kept well after the modification of sodium nitrate. Moreover, the XRD patterns of 0.2 wt%Rh/Al_2O_3 modified with 0–5 wt% Na were essentially the same, indicating that the impregnated $NaNO_3$ were well dispersed on the support. However, when the Na content in Rh/Al_2O_3 was higher than 7.5 wt%, the new or intensified peaks were appeared at 2θ of ca. 29°, 32°, 35°, 38°, 42°, and 48°. As the decomposition of $NaNO_3$ into $NaNO_2$ starts to occur at above 700 °C, and the catalyst was calcined at 500 °C, these peaks can be assigned to the diffractions of $NaNO_3$. Thus, the crystalline $NaNO_3$ was formed over the support when its content was at 7.5 wt% or above.

The pore structure properties of the catalysts are listed in Table 1. Both the surface areas and pore volumes of Rh/Al_2O_3 decreased obviously when it was modified with $NaNO_3$. Moreover, the higher the Na content in Rh/Al_2O_3, the lower the surface area and pore volume of the catalyst. Especially when $NaNO_3$ was crystallized (Na% >5 wt%), there appeared a sharp decrease. In the case of the average pore diameter, it was increased slightly with the increase of the Na content in Rh/Al_2O_3. From the pore size distribution shown in Fig. 4, the peak pore for all the catalysts was centered at 10 nm. These results indicated that the addition of $NaNO_3$ did not change the pore structure of Al_2O_3 even when crystallized $NaNO_3$ existed. Therefore, the decreased surface area and pore volume for the modified catalysts can be attributed to the block of some pores by sodium salt.

Table 1
The pore properties of the modified and unmodified 0.2 wt%Rh/Al_2O_3 catalysts.

Sample	BET surface area (m^2/g)	Pore volume (cm^3/g)	Average pore diameter (nm)
0.2 wt%Rh/Al_2O_3	221.7	0.76	13.8
2.5 wt%Na–0.2 wt%Rh/Al_2O_3	200.9	0.72	14.4
5 wt%Na–0.2 wt%Rh/Al_2O_3	181.7	0.67	14.8
7.5 wt%Na–0.2 wt%Rh/Al_2O_3	141.9	0.55	15.6
10 wt%Na–0.2 wt%Rh/Al_2O_3	119.2	0.48	16

Fig. 5 shows the effect of Na content in 0.2 wt%Rh/Al_2O_3 on DME conversion and H_2 yield. Irrespective of the Na contents, DME conversions were not influenced but H_2 yield did show some differences. The hydrogen yield increased to over 80% until the Na content was increased to 5 wt%, and began to decrease if the Na content was further increased. When the Na content was 10 wt%, H_2 yield was even lower than that without modification. Moreover, hydrogen yield over 10 wt%Na-0.2 wt%Rh/Al_2O_3 apparently decreased with the increase of TOS from 5 h while it was stable for the other catalysts. From the yields of C-containing product shown in Fig. 6, CO yield was apparently decreased while CO_2 yield was obviously increased when $NaNO_3$ was added into 0.2 wt%Rh/Al_2O_3. At the same time, increasing the Na content in 0.2 wt%Rh/Al_2O_3 from 2.5 to 10 wt% had only a slight influence on the yields of

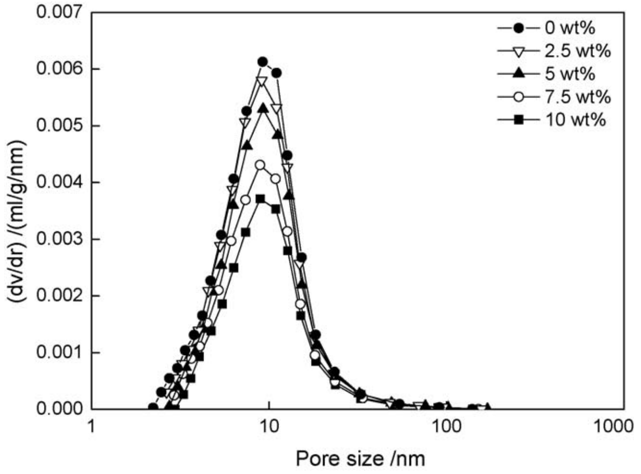

Fig. 4. The pore size distribution of 0.2 wt% Rh/Al_2O_3 modified with $NaNO_3$.

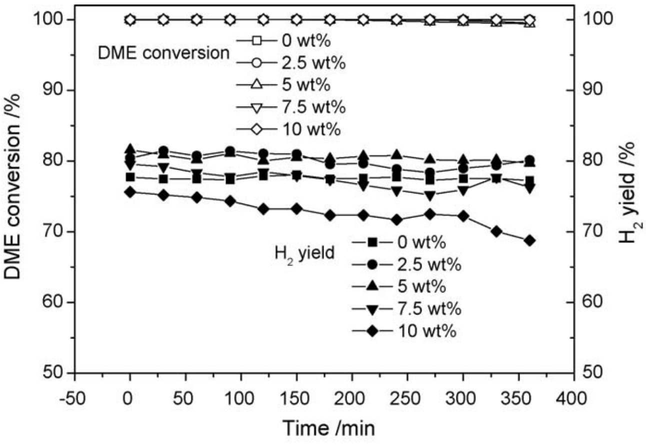

Fig. 5. DME conversion and H_2 yield over $NaNO_3$ modified 0.2 wt% Rh/Al_2O_3 combined with 6 wt% Ni/Al_2O_3 catalysts under the reaction conditions of $T = 700\ ^\circ C$, $P = 1$ atm, and $DME/O_2/Ar = 35/17/68$ ml/min.

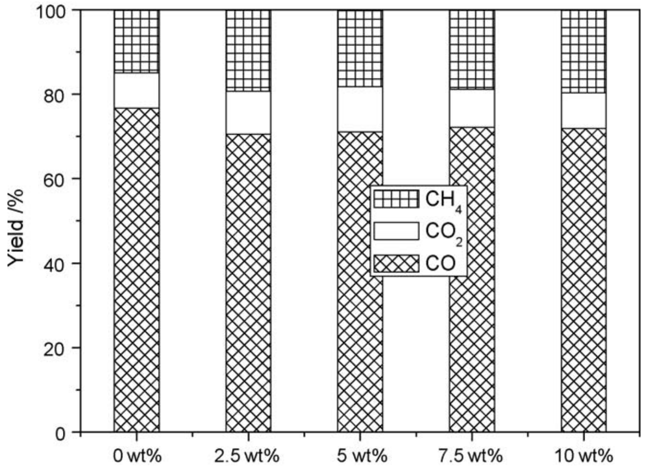

Fig. 6. Distribution of C-containing products over $NaNO_3$ modified 0.2 wt% Rh/Al_2O_3 combined with 6 wt% Ni/Al_2O_3 catalysts at TOS of 5 h under the reaction conditions of $T = 700\ ^\circ C$, $P = 1$ atm, $DME/O_2/Ar = 35/17/68$ ml/min.

CO and CO_2. In the case of CH_4 yields, it increased from 8.4% to 10.2% when the Na content in the catalyst was increased from 0 to 2.5 wt%. However, the CH_4 yield over 10 wt%Na–0.2 wt%Rh/Al_2O_3 was quite similar to that over 0.2 wt%Rh/Al_2O_3. The POD catalyst was supposed to play the role of suppressing the decomposition (Eq. (6)) and total oxidation (Eq. (7)) as well as catalyzing partial oxidation (Eq. (2)) of DME. The above results suggest that the addition of $NaNO_3$ decreased the ability of Rh/Al_2O_3 to suppress the decomposition of DME

$$CH_3OCH_3 = CH_4 + CO + H_2 \tag{6}$$

$$CH_3OCH_3 + 3O_2 = 2CO_2 + 3H_2O \tag{7}$$

In our previous works [10,11], it was found that the partial oxidation of DME was favored at a O_2/DME molar ratio of ca. 1. At a lower reaction temperature of 500 °C, Wang et al. [9] found that partial oxidation of DME over nickel-based catalyst was still favored even at a O_2/DME molar ratio of 1.5. However, even at a stoichiometric molar ratio of O_2/DME, the deep oxidation of DME (Eq. (7)) cannot be excluded [9]. Therefore, the increased CO_2 yields over $NaNO_3$-modified catalyst can be reasonably ascribed to the enhanced total oxidation of DME by the promotional effect of sodium nitrate. The promotional effect of sodium ion will be discussed together with the other alkali metal nitrates in a later part.

Table 2
Summary of the pore properties of 0.2 wt%Rh/Al_2O_3 modified with $LiNO_3$.

Sample	BET surface area (m^2/g)	Pore volume (cm^3/g)	Average pore diameter (nm)
2.5 wt%Li–0.2 wt%Rh/Al_2O_3	143.8	0.64	17.8
5 wt%Li–0.2 wt%Rh/Al_2O_3	91.7	0.47	20.7
7.5 wt%Li–0.2 wt%Rh/Al_2O_3	28.4	0.13	18.6

3.3. $LiNO_3$ modification of Rh/Al_2O_3

As the addition of $NaNO_3$ into Rh/Al_2O_3 had clear effects on hydrogen yields and C-containing product distribution, the modification of Rh/Al_2O_3 with $LiNO_3$ (Li content = 2.5, 5, and 7.5 wt%) were comparatively investigated for the titled reaction. Table 2 lists the pore structure properties of the $LiNO_3$ modified catalysts. Both the surface areas and pore volumes decreased sharply when the Li content in Rh/Al_2O_3 was increased, especially at a Li content of 7.5 wt%. Moreover, the pore size distribution was significantly influenced by $LiNO_3$ modification (Fig. 7). Though the pore size of 2.5 wt%Li–Rh/Al_2O_3 was also centered at ca. 10 nm, which is similar to that of the unmodified Rh/Al_2O_3, the peak pore sizes of 5 wt%Li–Rh/Al_2O_3 and 7.5 wt%Li–Rh/Al_2O_3 were shifted to 18 and 9 nm, respectively (Fig. 7). When the Li content in Rh/Al_2O_3 was 7.5 wt%, it is worthy to note that the surface area and pore volume was very low (Table 2) and the peak adsorption capacity was approaching to zero (Fig. 7), meaning that the pore structure of Rh/Al_2O_3 was collapsed with a larger amount of $LiNO_3$ added.

The catalytic performance of the $LiNO_3$ modified catalyst showed clear effects both on DME conversion and hydrogen yields (Fig. 8). With the increase of the Li content in Rh/Al_2O_3 from 0 to 5 wt%, both the DME conversion and hydrogen yield during the 6 h test were basically the same within the experimental errors. However, when the Li content was increased to be 7.5 wt%, the initial DME conversion was 100% and a higher initial hydrogen yield of 82% was obtained, indicating that higher $LiNO_3$ loading in Rh/Al_2O_3 is beneficial for the production of hydrogen at the initial reaction stage. However, both DME conversion and hydrogen yield obviously decreased with TOS, indicating that higher $LiNO_3$ loading reduced the stability of the catalyst. When the carbon-containing products were concerned, as shown in Fig. 9, the yields of CO_2 and CH_4 at TOS of 5 h were continuously increased with the increase of the Li content in the catalyst while CO yield was clearly decreased. This indicates that the DME decomposition

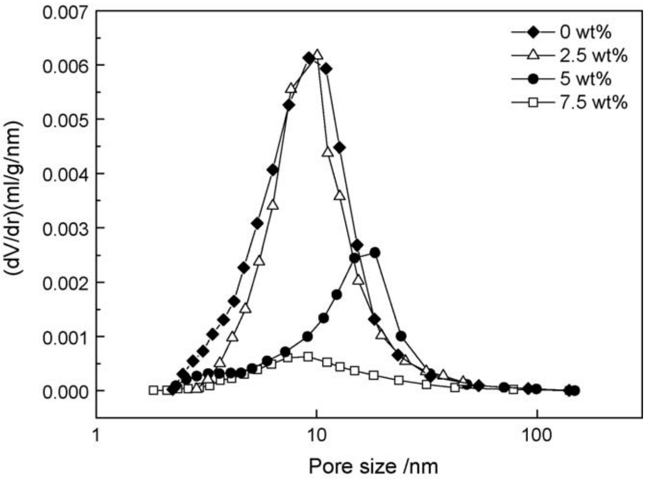

Fig. 7. The pore size distribution of 0.2 wt% Rh/Al_2O_3 modified with $LiNO_3$.

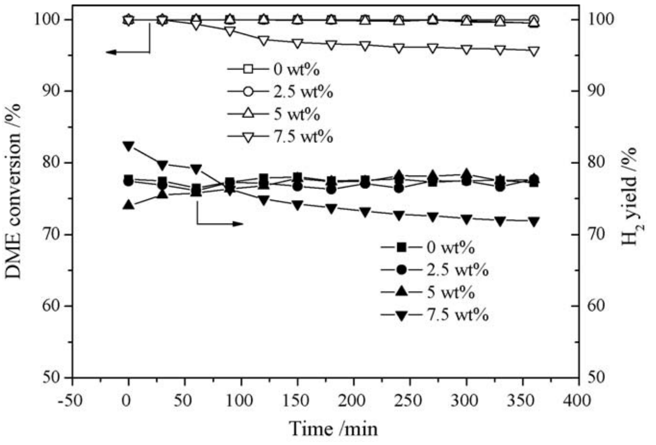

Fig. 8. Effect of $LiNO_3$ content in 0.2 wt%Rh/Al_2O_3 on the DME conversion and H_2 yield under the reaction conditions of $T = 700\ ^\circ C$, $P = 1$ atm, and DME/O_2/Ar = 35/17/68 ml/min.

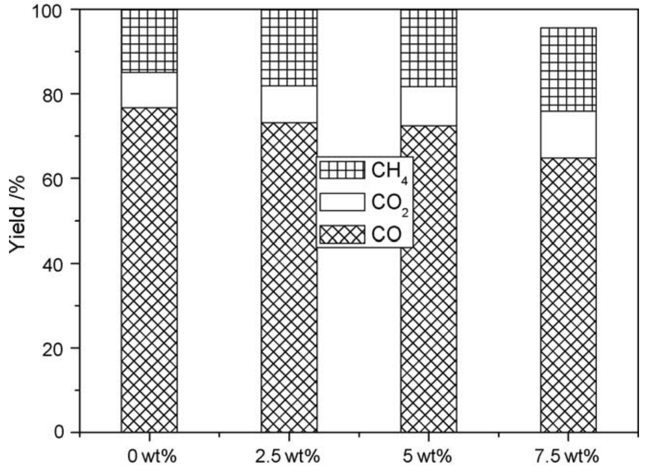

Fig. 9. Effect of $LiNO_3$ content in 0.2 wt%Rh/Al_2O_3 on the distribution of C-containing products at TOS of 5 h under the reaction conditions of $T = 700\ ^\circ C$, $P = 1$ atm, DME/O_2/Ar = 35/17/68 ml/min.

and deep oxidation of DME were favored over the catalyst modified with $LiNO_3$. Furthermore, this effect became more pronounced when the Li content was higher. To compare the product yields at different TOS, the results over 7.5 wt%Li–0.2 wt% Rh/Al_2O_3 are given in Fig. 10. With the increase of TOS, the yields of CH_4 and CO_2 showed a slightly continuous increase, which can be ascribed to the increased decomposition and deep oxidation of DME. Moreover, CO yield was clearly decreased paralleling to H_2 yield with the increase of TOS, suggesting that the catalyst for the partial oxidation of DME was deactivated based on Eq. (2). This deactivating behavior may be related to the decomposition of $LiNO_3$ under the reaction conditions. It is commonly known that $LiNO_3$ can be decomposed into Li_2O above 700 °C. Moreover, the formed Li_2O is a medium–strong base, which may produce stronger interactions with Al_2O_3 than that of $LiNO_3$. Consequently, the catalyst structure and the dispersion of Rh may be gradually changed with the increase of TOS leading to the deactivation of the catalyst for the titled reaction.

4. Discussion

From the above results, the modification of 0.2 wt%Rh/Al_2O_3 with $NaNO_3$ and $LiNO_3$ showed different promotional effects on the titled reaction. Moreover, the effects of alkali metal ions on the performance of the catalyst were clearly related to the content of the modifiers. It was reported that both the activity and stability of 0.5 wt%Rh/Al_2O_3 for the preferential oxidation of CO was significantly improved after modification of the catalyst with $NaNO_3$ [13]. The authors explained the results based on the functions of Na^+ in the aspect of: (1) increasing the dispersion of Rh on Al_2O_3; (2) regulating the interactions between Rh and Al_2O_3; (3) influencing the adsorption mode of CO by electronic functions of Na^+; and (4) changing the pore structure of the catalyst [13]. Additionally, the effect of all the alkali metal ions on the preferential oxidation of CO was comparatively studied, and a clear promotional effect was reported although the promoting mechanism is still unclear [14]. To disclose the promotional effects of different alkali metal ions on the titled reaction, 0.5 wt% Rh/Al_2O_3 promoted with 2.5 wt% of Li, Na, and K (in the form of nitrates), respectively, were comparatively investigated, and the results are summarized as follows.

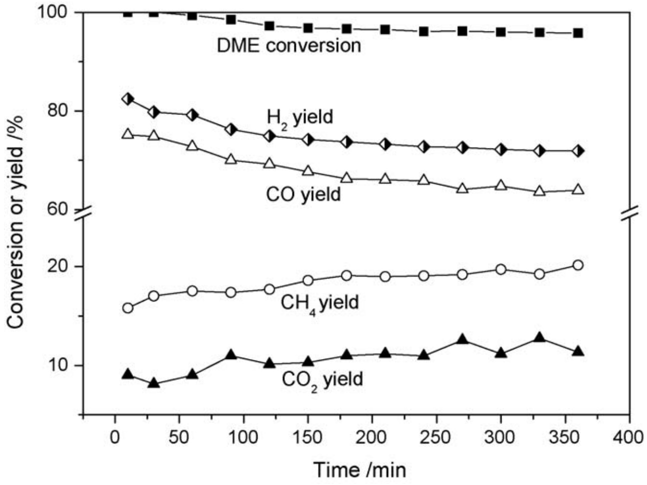

Fig. 10. DME conversion and yields of products over 7.5 wt%Li–0.2 wt%Rh/Al_2O_3 and 6 wt%Ni/Al_2O_3 composite catalysts under the reaction conditions of $T = 700\ ^\circ C$, $P = 1$ atm, and DME/O_2/Ar = 35/17/68 ml/min.

From the XRD patterns shown in Fig. 11, the main peaks were from the diffractions of Al_2O_3, and some weak peaks were due to the alkaline metal nitrates, indicating that the addition of $LiNO_3$, $NaNO_3$, or KNO_3 did not change the crystal structure of the support.

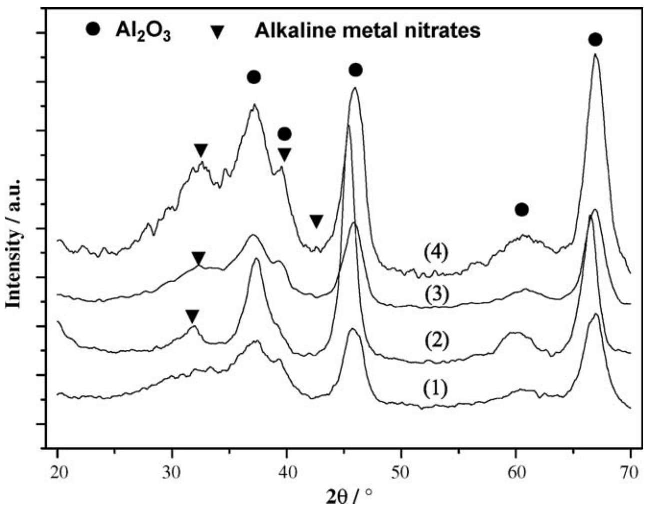

Fig. 11. XRD patterns of: (1) 0.2 wt%Rh/Al_2O_3, (2) 2.5 wt%Li–0.2 wt%Rh/Al_2O_3, (3) 2.5 wt%Na–0.2 wt%Rh/Al_2O_3, and (4) 2.5 wt%K–0.2 wt%Rh/Al_2O_3.

Table 3
The pore properties of 0.2 wt%Rh/Al_2O_3 modified with 2.5 wt% alkali metal nitrates.

Sample	BET surface area (m^2/g)	Pore volume (cm^3/g)	Average pore diameter (nm)
2.5 wt%Li–0.2 wt%Rh/Al_2O_3	143.8	0.64	17.8
2.5 wt%Na–0.2 wt%Rh/Al_2O_3	200.9	0.72	14.4
2.5 wt%K–0.2 wt%Rh/Al_2O_3	201.9	0.70	13.9

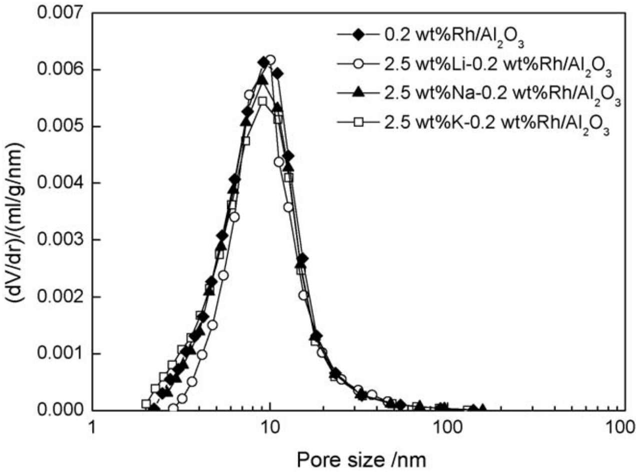

Fig. 12. Pore size distribution of 0.2 wt%Rh/Al_2O_3 modified with alkali metal nitrates.

As expected, there were no diffractions from Rh irrespective of the alkaline metal ions. The surface area, pore volume, and average pore size of Rh/Al_2O_3 modified with 2.5 wt% of Na and K were very similar, and only slightly deviated from those of the unmodified Rh/Al_2O_3 catalyst (Table 3). However, the surface area and pore volume of Rh/Al_2O_3 modified with 2.5 wt% of Li were significantly decreased while the average pore size was obviously increased. Moreover, from the pore size distribution shown in Fig. 12, all the catalysts showed quite similar pore size distributions although the peak maximum had minor differences. These results indicated that the addition of $LiNO_3$ made a clear change of the pore properties of the Rh/Al_2O_3 but a minor change with the addition of KNO_3 and $NaNO_3$.

The catalytic performances of Rh/Al_2O_3 modified with 2.5 wt% of Li, Na, and K are shown in Fig. 13. Although all the catalysts showed a DME conversion of 100% at the initial reaction stage of less than 1 h, DME conversion over Rh/Al_2O_3 modified with 2.5 wt% K obviously decreased while DME conversion over the remaining catalyst was still kept at 100% with the increase of TOS. In the case of hydrogen yield, the modification of Rh/Al_2O_3 with 2.5 wt% Na showed an obvious positive promotional effect. There was no effect on the hydrogen yield by the addition of 2.5 wt% Li into Rh/Al_2O_3. However, a negative effect by the addition of 2.5 wt% K into Rh/Al_2O_3 on the hydrogen yield was observed. Although the promoting effects of different alkaline metal nitrates on the titled reaction was not clear based on the available data, it may be caused from the electronic or structural promotions of alkaline metal ions. Qiu et al. [15] found that the addition of K^+ and Cs^+ leaded to a remarkable decrease in the catalytic activity of the Pt–Sn/γ-Al_2O_3 for the dehydrogenation of long-chain paraffins, and they ascribed the deactivation of the catalyst to the change of the metal-support interactions induced from the basicity of the alkaline metals. Chen et al. [16] found that the addition of K^+ promoter into Rh/Al_2O_3 weakened the adsorption intensity of CO on Rh. Based on these literature results, the quite different promotional effects of Li^+, Na^+, and K^+ on the catalytic performance of Rh/Al_2O_3 for the titled reaction may be mainly caused by the electronic effects of alkaline metal ions on Rh. In fact, the basic alkali metal ions are easy to interact with acidic γ-Al_2O_3, and the interaction intensity is in the order of basicity: $K^+ > Na^+ > Li^+$. The interaction between alkali metal ions and Al_2O_3 will consequently affect the Rh–Al_2O_3 interaction, which eventually affects the adsorption behavior of the reactants, products, and/or reaction intermediates. It was reported that K^+ over Rh–K/Al_2O_3 catalyst showed some electron-donating properties, which weakened the CO adsorption on Rh and increased the activity for the oxidation of CO to CO_2 [16]. In our work, the CO yield over 2.5 wt% K modified Rh/Al_2O_3 was much lower than that over 2.5 wt% Li or Na modified Rh/Al_2O_3 (Fig. 14), which is consistent to the above viewpoint. Thus, this may be the main reason for the different catalytic performances of Rh/Al_2O_3 modified with the alkaline metal ions.

Irrespective of the alkaline metal ions, a declined hydrogen yield was observed when the content of the alkaline metal ions was at a higher level. Moreover, significantly lower pore volume and surface area together with an obviously higher average pore size were obtained at a higher content of the modifier over Rh/Al_2O_3. Based on these facts, the pore properties of the catalyst induced by the alkaline metal ions may also play a role in determining the promotional effects of the modifiers.

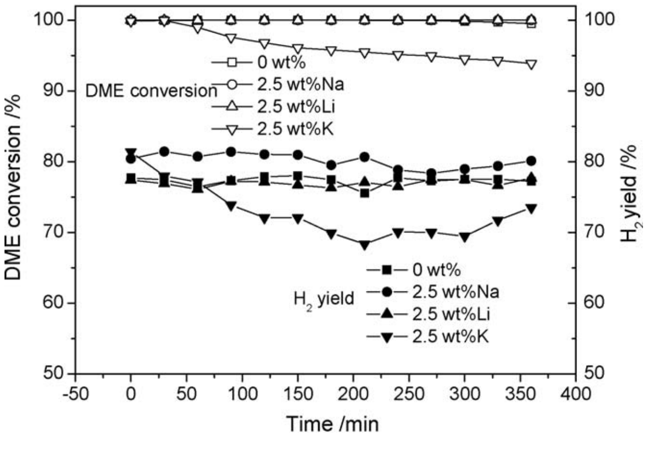

Fig. 13. DME conversion and H_2 yield over composite catalysts composed of 0.2 wt%Rh/Al_2O_3 modified with alkali metal nitrates and 6 wt%Ni/Al_2O_3 under the reaction conditions of $T = 700$ °C, $P = 1$ atm, and DME/O_2/Ar = 35/17/68 ml/min.

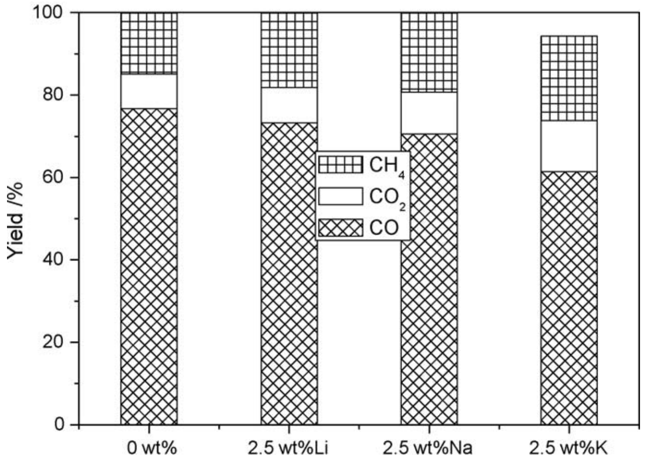

Fig. 14. Distribution of C-containing products over composite catalysts composed of 0.2 wt%Rh/Al_2O_3 modified with alkali metal nitrates and 6 wt%Ni/Al_2O_3 at TOS of 5 h under the reaction conditions of $T = 700$ °C, $P = 1$ atm, and DME/O_2/Ar = 35/17/68 ml/min.

5. Conclusions

Based on the above results and discussion, the following conclusions can be drawn.

(1) Over the composite catalyst composed of 6 wt%Ni/Al_2O_3 as a reforming catalyst and noble metal/Al_2O_3 as a POD catalyst, Rh/Al_2O_3 showed better hydrogen yield than Pt/Al_2O_3 although 100% DME conversion was achieved in both cases.

(2) For the Na–Rh/Al_2O_3 catalyst, the pore volume and surface area continuously decreased with the increase of Na content over the catalyst. A much sharper decrease of the pore volume and surface area was observed in the case of Rh/Al_2O_3 modified with $LiNO_3$. However, the bulk structure of Al_2O_3 was still reserved irrespective of the contents of the alkaline metal nitrates. For the modified or unmodified Rh/Al_2O_3 catalysts, the absence of XRD peaks of Rh species indicated a well dispersion of Rh over Al_2O_3.

(3) An increased performance of Na–Rh/Al_2O_3 for the titled reaction was obtained at an optimal Na content of 2.5–5 wt%. However, there was basically no effect by adding less than 5 wt% of Li (in the form of $LiNO_3$) into Rh/Al_2O_3 on the activity and stability of the catalyst, but a negative effect at a higher Li content of 7.5 wt%. In the case of KNO_3, an obvious decrease of DME conversion and hydrogen yield was observed by adding 2.5 wt% of K into Rh/Al_2O_3. These promotional effects of alkaline metal ions on Rh/Al_2O_3 were tentatively explained mainly as the different electronic effects of Li^+, Na^+, and K^+ on Rh/Al_2O_3.

Acknowledgements

This work is financially supported by National Natural Science Foundation of China (Grant No. 20603015), and the Scientific Research Foundation for the Returned Overseas Chinese Scholars, State Education Ministry.

References

[1] K. Faungnawakij, N. Shimoda, T. Fukunaga, R. Kikuchi, K. Eguchi, Appl. Catal. A: Gen. 341 (1–2) (2008) 139.
[2] M. Nilsson, P. Jozsa, L.J. Pettersson, Appl. Catal. B: Environ. 76 (2007) 42.
[3] V.V. Galvita, G.L. Semin, V.D. Belyaev, T.M. Yurieva, V.A. Sobyanin, Appl. Catal. A: Gen. 216 (1–2) (2001) 85.
[4] K. Takeishi, H. Suzuki, Appl. Catal. A: Gen. 260 (1) (2004) 111.
[5] T. Mathew, Y. Yamada, A. Ueda, H. Shioyama, T. Kobayashi, Appl. Catal. A: Gen. 286 (1) (2005) 11.
[6] T.A. Semelsberger, K.C. Ott, R.L. Borup, H.L. Greene, Appl. Catal. B: Environ. 65 (3–4) (2006) 291.
[7] K. Faungnawakij, Y. Tanaka, N. Shimoda, T. Fukunaga, S. Kawashima, R. Kikuchi, K. Eguchi, Appl. Catal. A: Gen. 304 (2006) 40.
[8] T. Kawabata, H. Matsuoka, T. Shishido, D. Li, Y. Tian, T. Sano, K. Takehira, Appl. Catal. A: Gen. 308 (2006) 82.
[9] S. Wang, T. Ishihara, Y. Takita, Appl. Catal. A: Gen. 228 (2002) 167.
[10] Q. Zhang, X. Li, K. Fujimoto, K. Asami, Appl. Catal. A: Gen. 288 (2005) 169.
[11] Q. Zhang, X. Li, K. Fujimoto, K. Asami, Catal. Lett. 102 (3–4) (2005) 197.
[12] J. Zou, Y. Zhang, C. Liu, Inter. J. Hydrogen Energy 32 (8) (2007) 958.
[13] F. Wang, G. Lu, Chin. J. Catal. 28 (1) (2007) 27.
[14] Y. Minemura, M. Kuriyama, S. Ito, K. Tomishige, K. Kunimori, Catal. Commun. 7 (9) (2006) 623.
[15] A. Qiu, Y. Fan, Y. Ma, P. Wu, Y. Chen, Chin. J. Catal. 22 (4) (2001) 343.
[16] G. Chen, S. Li, Q. Yuan, F. Jiao, Chin. J. Catal. 26 (9) (2005) 809.